JACS
JOURNAL OF THE AMERICAN CHEMICAL SOCIETY
Article
pubs.acs.org/JACS

Structural Evolution of Carbon Dioxide under High Pressure

Cheng Lu,[†,‡,§] Maosheng Miao,*[,§,∥] and Yanming Ma*[,†,§]

[†]State Key Laboratory of Superhard Materials, Jilin University, Changchun 130012, People's Republic of China
[‡]Department of Physics, Nanyang Normal University, Nanyang 473061, People's Republic of China
[§]Beijing Computational Science Research Center, Beijing 10084, People's Republic of China
[∥]Materials Department and Materials Research Laboratory, University of California, Santa Barbara, California 93106-5050, United States

Supporting Information

ABSTRACT: Using an efficient structure search method based on a particle swarm optimization algorithm, we study the structural evolution of solid carbon dioxide (CO_2) under high pressure. Our results show that, although it undertakes many structural transitions under pressure, CO_2 is quite resistive to structures with C beyond 4-fold coordination. For the first time, we are able to identify two 6-fold structures of solid CO_2 with *Pbcn* and $Pa\bar{3}$ symmetries that become stable at pressures close to 1 TPa. Both structures consist of a network of C−O octahedra, showing hypervalence of the central C atoms. The C−O bond length varies from 1.30 to 1.34 Å at the 4-fold to 6-fold transition, close to the C−O distance in the transition state of a corresponding S_N2 reaction. It has been a longstanding and challenging objective to stabilize C in a hypervalent state, particularly when it is bonded with nonmetallic elements. Most of the work so far has focused on synthesizing organic molecules with a high coordination number of C. Our results provide a good measure of the resistivity of C toward forming hypervalent compounds with nonmetallic elements and of the barrier of reaction involving C−O bonds.

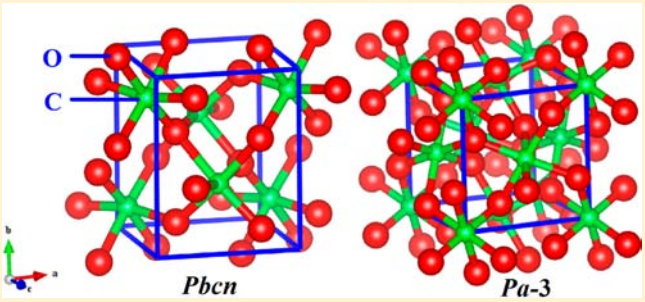

1. INTRODUCTION

CO_2 is a typical nonpolar molecule containing polar bonds. Its structural changes under pressure involve the breaking and the forming of C−O bonds and have been intensely studied over the past two decades.[1−8] Furthermore, CO_2 is one of the most important materials of the giant planets in the solar system, such as Mars and Venus.[1] The study of its high-pressure structural changes provides crucial knowledge for planetary science and geophysics.[2,3]

Previous theoretical and experimental studies on CO_2 have focused on the molecular phases and their transition to 4-fold extended solids.[3−8] About eight solid phases of CO_2 have been identified so far.[7] Aoki et al. presented the X-ray diffraction (XRD) measurements on solid CO_2 at room temperature and showed the powder pattern of the orthorhombic high pressure *Cmca* phase, which supersedes the low-pressure cubic $Pa\bar{3}$ phase at about 10 GPa.[9] Later on, Yoo et al. characterized the crystal structure of CO_2-II ($P4_2/mnm$) and discussed tetragonal to orthorhombic (*Pnnm*) distortion by angle-resolved XRD under pressures up to 100 GPa and at elevated temperatures.[10] On the basis of a large number of resistive- and laser-heating experiments using membrane diamond-anvil cells, they proposed the relationship between the molecular and extended phases at high pressures and temperatures.[7] Although extensive studies have been performed for exploring the high-pressure phases of solid CO_2, the pressure range studied to date is limited to about 500 GPa,[11] which is lower than for other simple molecular solids, for instance: H_2, >5 TPa;[12] O_2, >9 TPa;[13,14] H_2O, >4 TPa.[15] So far, no 6-fold structure has been observed experimentally or predicted theoretically. Of note, the 4-fold to 6-fold structural transition happens at 25−30 GPa for SiO_2. The phase diagram and high-pressure behavior of solid CO_2 is still controversial: in particular, for nonmolecular phases. Many important questions still remain: among them, the most intriguing one is whether at sufficiently high pressure CO_2 can form 6-fold structures containing hypervalent C atoms.

Solid CO_2 can be used as a prototype compound for studying the hypervalency of light elements in an extended solid. The octet rule in chemistry states that elements gain or lose electrons to attain an electron configuration of the nearest noble gas.[16] It has been known for a long time that this rule is not always valid.[17] Elements such as P, S, and Si can become hypervalent in molecules by accommodating more than eight covalent electrons while forming bonds with nonmetallic elements such as O and F.[18,19] Several compounds containing hypercoordinated C atoms bonded with metallic elements have been found, including for example, C-centered FeMo-co in nitrogenase and octahedral C coordinated by six Au atoms in

Received: May 14, 2013
Published: September 4, 2013

   dx.doi.org/10.1021/ja404854x | J. Am. Chem. Soc. 2013, 135, 14167−14171

the polynuclear metal clusters $[(LAu)_6C]^{2+}$.[20,21] A few C–metal clusters such as octahedral CLi_6 have been predicted to contain hypervalent C atoms.[22] However, these C–metal systems appearing largely on molecules or clusters are electron-deficient carbocations and/or are stabilized by metal–metal cage interactions.[23] Despite much effort, the C atoms are found to be very resistive to become hypervalent while being bonded with nonmetallic elements, and the search for organic molecules and solid compounds containing hypervalent C atoms bonded with nonmetallic elements has so far been scarcely successful.[18,24] The search for hypervalent C in solids is not only important for establishing a longstanding concept but also very valuable for understanding the electronic and atomic processes of chemical reactions, since hypervalent C often represents the C atoms going through transition states of reactions. Note that, in the present work, we take a very different approach. Instead of proposing molecules containing hypervalent C atoms, we focus on driving C atoms in the solid to a hypervalent state by physical forces of hydrostatic pressure.

In order to systematically study the structure evolution of CO_2 under high pressure, and especially to examine the possibility of attaining hypervalent C and study the chemical nature of its bonding with neighboring atoms, we here present extensive structure searches to explore the high-pressure structures of solid CO_2 up to 1200 GPa, using our developed CALYPSO algorithm for crystal structure predictions.[25−28] We are able to predict two novel high-pressure phases, *Pbcn* and $Pa\bar{3}$, both featuring 6-fold coordination of C atoms, revealing that hypervalent C can be achieved in solids but is limited to extremely high pressure.

2. COMPUTATIONAL METHODS AND DETAILS

Our structure prediction is based on a global minimum search of the free energy surfaces obtained by ab initio total-energy calculations, through CALYPSO (crystal structure analysis by particle swarm optimization) methodology and its same-name code.[25−28] The significant feature of this methodology is the capability of predicting the stable structure with only the knowledge of the chemical composition at given external conditions (for example, pressure). It has been successful in correctly predicting structures for various systems, including elements and binary and ternary compounds.[14,15,29−34] The details of this search algorithm have been described elsewhere.[25−28] The underlying ab initio structural relaxations and electronic calculations have been carried out using density functional theory within the Perdew–Burke–Ernzerhof (PBE) exchange correlation as implemented in the VASP (Vienna ab initio simulation package) code.[35] The frozen-core all-electron projector-augmented wave method has been adopted, with $2s^22p^2$ (cutoff radius 1.5 au) and $2s^22p^4$ (cutoff radius 1.52 au) treated as valence electrons for C and O, respectively. The cutoff energy of 1200 eV for the expansion of the wave function into plane waves and fine Monkhorst–Pack k meshes have been chosen to ensure that all the enthalpy calculations are well converged to better than 1 meV/atom. The accuracy of the total energies obtained within the framework of density functional theory is in many cases sufficient to predict the stability of structures. The phonon calculations have been carried out by using a supercell approach as implemented in the PHONOPY code.[36]

3. RESULTS AND DISCUSSION

The structures found by CALYPSO searches in the pressure range from 0 to 1200 GPa can be categorized into three kinds: molecular and 4-fold and 6-fold coordinated structures (Figure 1). All earlier known structures, experimentally and theoretically, were successfully reproduced by our current structure searches (see Figures S1 and S2 in the Supporting Information), validating our methodology in application to solid CO_2. The enthalpies of various structures under pressure are shown in Figure 2. Figure 3 shows the pressure evolution of the unit cell volume of solid CO_2 together with the experimental results.[37−39] The agreement between the experimental $P–V$ data and the calculated results are excellent for both the $Pa\bar{3}$ and $P4_2/mnm$ phases (Figure 3). At ambient pressure, CO_2 molecules condense in an optically isotropic molecular crystal in a cubic $Pa\bar{3}$ structure (commonly known as dry ice),[9] with CO_2 molecules located on face-centered cubic (FCC) lattice sites (Figure 1a). At 10.3 GPa, this molecular phase transforms to a $P4_2/mnm$ structure, which is also a molecular crystal (Figure 1b).[40] The calculated transition pressure is in good agreement with the experimental result of 11 GPa and computational result of 8.9 GPa.[9,40] Another interesting molecular crystal structure predicted takes a *Pbcn* symmetry (Figure S1). At low pressure, it is only about 40 meV/atom higher in enthalpy than the $Pa\bar{3}$ structure (Figure 2a).

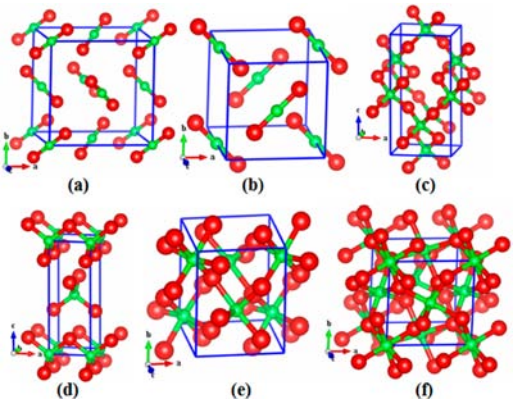

Figure 1. Crystal structures of solid CO_2: (a) $Pa\bar{3}$ molecular phase; (b) $P4_2/mnm$ molecular phase; (c) $I\bar{4}2d$ 4-fold coordinated polymeric phase; (d) $P4_2/nmc$ 4-fold coordinated polymeric phase; (e) *Pbcn* 6-fold coordinated polymeric phase; (f) $Pa\bar{3}$ 6-fold coordinated polymeric phase. In all parts the O atoms are large and red and the C atoms are small and green.

With increasing pressure, CO_2 transforms to various forms of nonmolecular extended solids.[7] At a pressure of 17.9 GPa (Figure 2a), the $P4_2/mnm$ structure undergoes a transition to a tetragonal structure with space group $I\bar{4}2d$, which remains stable up to 285 GPa (Figure 1c). This structure has been proposed in an earlier work, which predicted a $P4_2/mnm \rightarrow I\bar{4}2d$ transition pressure at 18.6 GPa.[40] In the $I\bar{4}2d$ structure, C and O atoms form CO_4 tetrahedral units linked by O atoms at the corners. The C–O bond distance is 1.352 Å, which is slightly shorter than a typical C–O single bond (1.43 Å) but significantly longer than a C=O double bond (1.168 Å).[41,42]

At 285 GPa (Figure 2b), the $I\bar{4}2d$ structure undergoes a transition into a two-dimensional layered $P4_2/nmc$ structure containing two CO_2 units per cell (Figure 1d). The $P4_2/nmc$ structure has a two-dimensional network consisting of tetrahedrons, with C atoms siting at the center of tetrahedrons and O atoms at the corner in a bridge position between two C atoms. This structure is far different from the other nonmolecular structures, which are composed of a three-dimensional network of tetrahedrons: e.g., the $P4_12_12$ structure (Figure S2, Supporting Information). The layered feature of the $P4_2/nmc$ structure gives rise to a more open interstitial region between the O atoms, allowing the accommodation of the 2p

dx.doi.org/10.1021/ja404854x | J. Am. Chem. Soc. 2013, 135, 14167−14171

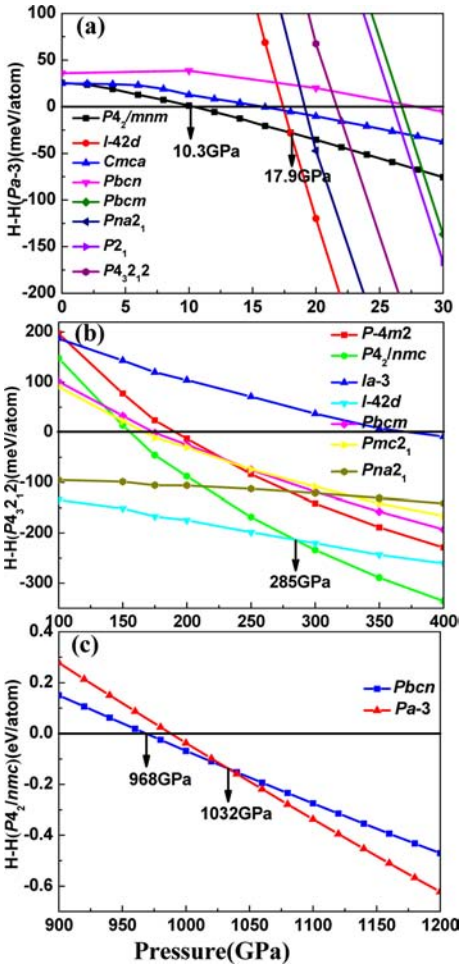

Figure 2. Enthalpy–pressure relations for solid CO_2: (a) in the low-pressure region (enthalpies are shown per atom and relative to the molecular $Pa\bar{3}$ structure); (b) in the high-pressure region (enthalpies are shown per atom and relative to the 4-fold coordinated $P4_32_12$ structure); (c) in the ultrahigh-pressure region (enthalpies are shown per atom and relative to the 4-fold coordinated $P4_2/nmc$ structure).

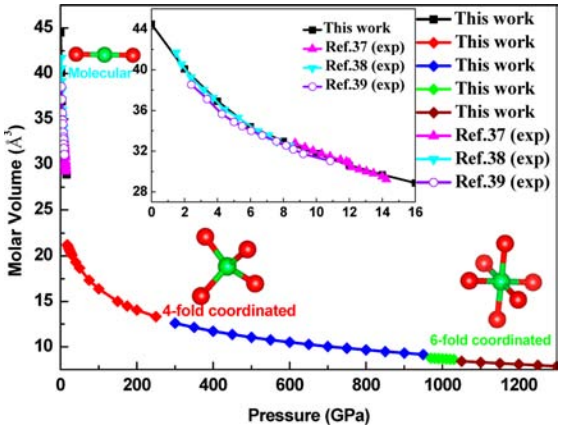

Figure 3. Volume vs pressure data for solid CO_2. The upward-pointing and downward-pointing triangles for the $Pa\bar{3}$ phase are from refs 37 and 38, respectively. The cycle for the $P4_2/mnm$ phase is from ref 39. The diamonds are the theoretical data for the high-pressure phases.

lone-pair electrons on O atoms. This $P4_2/nmc$ structure was first reported as a compression product of phase III by Serra et al.[11] However, there are so far no experimental and theoretical reports available related to the stability range of the $P4_2/nmc$ structure at high pressures. The present calculations suggest that the layered $P4_2/nmc$ structure is stable from 285 to 968 GPa. Our structure search also obtained the *Cmca* structure proposed by Aoki et al.[9] and Yoo et al.[10] However, it is metastable with respect to the $I\bar{4}2d$ and $P4_2/nmc$ structures.

Our calculations show that the transition from a 4-fold structure to a 6-fold structure only takes place at a pressure close to 1000 GPa. Two 6-fold structures are found, having *Pbcn* (Figure 1e) and $Pa\bar{3}$ (Figure 1f) structures, respectively. As shown in Figure 2c, the transition from the 4-fold $P4_2/nmc$ structure to the 6-fold *Pbcn* structure occurs at 968 GPa and to the $Pa\bar{3}$ structure at 1032 GPa. The dynamic stabilities of both *Pbcn* and $Pa\bar{3}$ structures are verified by phonon calculations, which show no imaginary frequency in the entire Brillouin zone (see Figures S6(a) and S7(a) in the Supporting Information). Both structures consist of a three-dimensional network of distorted octahedrons. However, the octahedra in the *Pbcn* structure are both corner and edge sharing, whereas the octahedra in the $Pa\bar{3}$ structure are only corner sharing. In the *Pbcn* structure, two C atoms and two O atoms of the neighboring CO_6 octahedrons form a parallelogram with two C–O bonds of 1.30 and 1.34 Å and angles of 96.35 and 83.65°. The large variation of the bond lengths and angles indicates a large deviation from an ideal octahedron in the *Pbcn* structure. In contrast, the C–O pairs in neighboring octahedra of the $Pa\bar{3}$ structure form ideal six-membered rings, and the C atoms in the $Pa\bar{3}$ structure bond equally with six neighboring O atoms with a C–O bond length of 1.31 Å, indicating the C–O octahedra are in an absolutely ideal geometry. The higher symmetry of the $Pa\bar{3}$ structure can also be seen from the simulated XRD patterns. As shown in Figure S8 (in the Supporting Information), the $Pa\bar{3}$ structure exhibits only one significant peak in the range of 5–13°, whereas *Pbcn* shows two. As a matter of fact, we found that, while changing from molecular crystal to 4-fold and 6-fold extended structures, the number of XRD peaks decreases substantially.

Interestingly, both symmetry groups ($Pa\bar{3}$ and *Pbcn*) are also found in molecular phases in the low-pressure range (Figure S1, Supporting Information). A careful inspection revealed that there are close relations between the low-pressure molecular structures and the 6-fold high-pressure polymeric structures within the same symmetry group. By examining the atomic positions, we are able to identify transition paths from one structure to the other (Figure 4). This significant similarity of the molecular crystal structure to its high-pressure 6-fold structure is probably due to the fact that the interaction of the O lone pairs with C orbitals resemble the much stronger C–O interaction under higher pressure that leads to a hypervalent state of C.

Despite the fact that C atoms in these 6-fold structures are hypervalent, they form strong covalent bonds with the six neighboring O atoms. As shown by the band structures (Figure 5), these two structures are insulating, with band gaps of 4.6 and 7.3 eV for the *Pbcn* and $Pa\bar{3}$ structures, respectively. The projected density of states reveals that the states close to the valence band maximum (VBM) are mainly O 2p, whereas the states around the conduction band minimum (CBM) consists of more C 2p orbitals. The strong covalent bonding between C and neighboring O atoms can also be seen from the electron-localized functions (ELF) (Figure 6). In the cases of molecular crystals ($Pa\bar{3}$ and $P4_2/mnm$ phases), the localization of the electrons around O atoms can be easily seen (Figure S11,

dx.doi.org/10.1021/ja404854x | J. Am. Chem. Soc. 2013, 135, 14167–14171

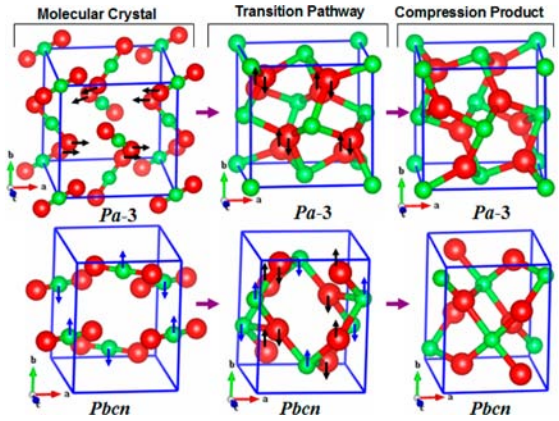

Figure 4. Predicted phase relationships in the molecular to nonmolecular transitions of solid CO_2.

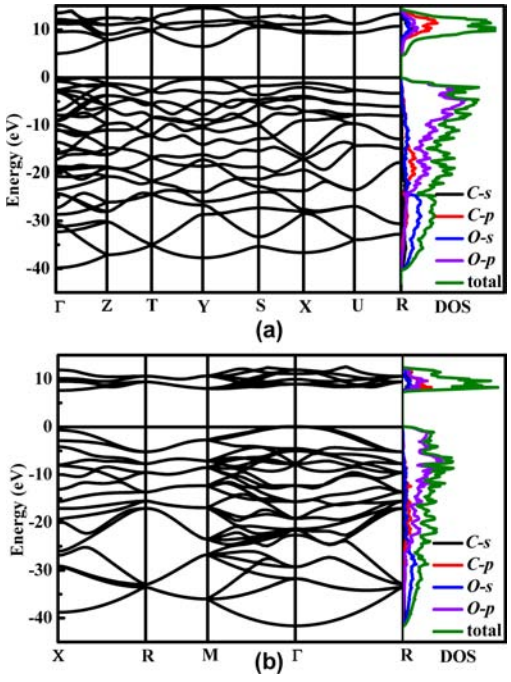

Figure 5. Electronic band structures and densities of states (DOS) for the 6-fold coordinated (a) *Pbcn* phase at 1000 GPa and (b) $Pa\bar{3}$ phase at 1100 GPa.

Supporting Information). They represent the O 2p lone pair states. Large ELF basins also exist between the C and O atoms, showing the strong covalent bonds. Although the localization of the electrons becomes weaker for extended structures, including both 4-fold and 6-fold structures, they still indicate strong single covalent bands between the neighboring C and O atoms.

As in many compounds including transition-metal oxides, the atoms at the center of the octahedron are in sp^3d^2 hybridization. However, by checking the projected density of states of *Pbcn* and $Pa\bar{3}$ structures, we found that there are negligible C d components in the states close to the VBM and the CBM. This is due to the fact that the valence electrons in C atoms are in 2p states that do not have a corresponding d orbital. The closest d level is 3d, which is much higher in energy. This is one reason that C is strongly resistant to become hypervalent. Without the involvement of the d orbitals, the propensity of forming a hypervalent state is proportional to

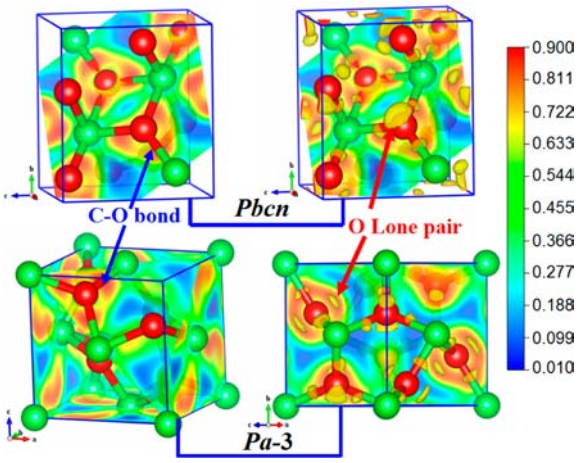

Figure 6. Electron localization functions (ELF) of *Pbcn* and $Pa\bar{3}$ structures at 1000 GPa.

the inclination of sharing the electrons. For example, in valence bond theory, the hypervalent state of SF_6 can be viewed as the resonance of different $SF_4^{2+} + 2F^-$ configurations.[43] Therefore, the less inclination there is to lose electrons, the harder it is to form hypervalent compounds. This is the physical origin why CO_2 is significantly more resistive to become hypervalent than SiO_2. Furthermore, we also notice that the O atoms in these two 6-fold structures are equally bonded to three neighboring C atoms (Figure 6). The three C−O bonds are in the same plane, indicating that the O is in sp^2 hybridization. This is different from the case for most of the organic molecules, including those proposed for hypervalent C, in which O atoms are typically in sp^3 hybridization. The C−O bond length varies from 1.30 to 1.34 Å, very close to the C−O distances (1.30−1.36 Å) in the transition state of a S_N2 reaction.[24] The sp^2 hybridization of O should in principle shorten the C−O bond (1.43 Å),[24] consistent with the compressive nature of the C−O bond in 6-fold structures, whose length varies from 1.30 to 1.34 Å, nearly identical with the C−O distances in the transition state of a S_N2 reaction.[24]

4. SUMMARY

In the present work, we systematically studied the structural evolution of CO_2 under high pressure in search of hypervalent C. By use of the CALYPSO structure searching algorithm, we are able to identify two 6-fold structures of CO_2 in *Pbcn* and $Pa\bar{3}$ space groups, both consisting of C−O octahedra. These structures are stable at a pressure close to 1 TPa, showing the strong resistivity of C toward the hypervalent state. Due to the distortion, the C−O bond lengths vary from 1.30 to 1.34 Å, all significantly smaller than the usual C−O bond length of 1.43 Å under ambient conditions. However, these bond lengths are close to the C−O distances in an S_N2 reaction that involves C−O bonds. Our results suggest that the hypervalent C can only be stabilized with greatly suppressed C−O bonds either in solid compounds or in deliberately designed molecules. In addition, we confirmed the known structures of molecular phases and 4-fold phases of CO_2 and have thoroughly discussed their properties and high-pressure structural transitions.

dx.doi.org/10.1021/ja404854x | J. Am. Chem. Soc. 2013, 135, 14167−14171

■ ASSOCIATED CONTENT

Supporting Information

Text, figures, and tables giving the high-pressure phases for solid carbon dioxide and physical properties calculated at different pressures. This material is available free of charge via the Internet at http://pubs.acs.org.

■ AUTHOR INFORMATION

Corresponding Authors

miaoms@gmail.com.
mym@jlu.edu.cn; mym@calypso.cn

Notes

The authors declare no competing financial interest.

■ ACKNOWLEDGMENTS

This research was supported by the China 973 Program (2011CB808200), the Natural Science Foundation of China under grants 11274136, 11104104, 11025418, 11304167, 11304141, and 91022029, the 2012 Changjiang Scholars Program of China, Changjiang Scholar and Innovative Research Team in University (IRT1132), the Postdoctoral Science Foundation of China under grant 20110491317, and the research fund of Key Laboratory of Surface Physics and Chemistry (SPC201103). M.M. thanks the ConvEne-IGERT Program (NSF-DGE0801627) and the MRSEC program (NSF-DMR1121053).

■ REFERENCES

(1) Liu, L. *Nature* **1983**, *303*, 508−509.
(2) Litasov, K. D.; Goncharov, A. F.; Hemley, R. J. *Earth Planet. Sci. Lett.* **2011**, *309*, 318−323.
(3) Sun, J.; Klug, D. D.; Martonak, R.; Montoya, J. A.; Lee, M. S.; Scandolo, S.; Tosatti, E. *Proc. Natl. Acad. Sci. U.S.A.* **2009**, *106*, 6077−6081.
(4) Datchi, F.; Mallick, B.; Salamat, A.; Ninet, S. *Phys. Rev. Lett.* **2012**, *108*, 125701/1−125701/5.
(5) Sengupta, A.; Kim, M.; Yoo, C. S.; Tse, J. S. *J. Phys. Chem. C* **2012**, *116*, 2061−2067.
(6) Santoro, M.; Gorelli, F.; Haines, J.; Cambon, O.; Levelut, C.; Garbarino, G. *Proc. Natl. Acad. Sci. U.S.A.* **2011**, *108*, 7689−7692.
(7) Iota, V.; Yoo, C. S.; Klepeis, J. H.; Jenei, Z.; Evans, W.; Cynn, H. *Nat. Mater.* **2007**, *6*, 34−38.
(8) Yoo, C. S.; Cynn, H.; Gygi, F.; Galli, G.; Iota, V.; Nicol, M.; Carlson, S.; Hausermann, D.; Mailhiot, C. *Phys. Rev. Lett.* **1999**, *83*, 5527−5530.
(9) Aoki, K.; Yamawaki, H.; Sakashita, M.; Gotoh, Y.; Takemura, K. *Science* **1994**, *263*, 356−358.
(10) Yoo, C. S.; Kohlmann, H.; Cynn, H.; Nicol, M. F.; Iota, V.; LeBihan, T. *Phys. Rev. B* **2002**, *65*, 104103/1−104103/6.
(11) Serra, S.; Cavazzoni, C.; Chiarotti, G. L.; Scandolo, S.; Tosatti, E. *Science* **1999**, *284*, 788−790.
(12) Liu, H. Y.; Wang, H.; Ma, Y. M. *J. Phys. Chem. C* **2012**, *116*, 9221−9226.
(13) Sun, J.; Martinez-Canales, M.; Klug, D. D.; Pickard, C. J.; Needs, R. J. *Phys. Rev. Lett.* **2012**, *108*, 045503/1−045503/5.
(14) Zhu, L.; Wang, Z.; Wang, Y.; Zou, G.; Mao, H. K.; Ma, Y. M. *Proc. Natl. Acad. Sci. U.S.A.* **2012**, *109*, 751−753.
(15) Wang, Y. C.; Liu, H. Y.; Lv, J.; Zhu, L.; Wang, H.; Ma, Y. M. *Nat. Commun.* **2011**, *2*, 563/1−563/5.
(16) Maugh, T. H. *Science* **1983**, *222*, 403−403.
(17) Liu, X. F.; Matsuishi, S.; Fujitsu, S.; Ishigaki, T.; Kamiyama, T.; Hosono, H. *J. Am. Chem. Soc.* **2012**, *134*, 11687−11694.
(18) Akiba, K. Y. *Chemistry of Hypervalent Compounds*; Wiley-VCH: Weinheim, Germany, 1998; pp 1−40.
(19) Olah, G. A.; Prakash, G. K. S.; Wade, K.; Molnár, Á.; Williams, R. E. *Hypercarbon Chemistry*, 2nd ed.; Wiley: Hoboken, NJ, 2011; pp 223−274.
(20) Dance, I. *Dalton Trans.* **2012**, *41*, 4859−4865.
(21) Häberlen, O. D.; Schmidbaur, H.; Rösch, N. *J. Am. Chem. Soc.* **1994**, *116*, 8241−8248.
(22) Schleyer, P. v. R.; Wurthwein, E. U.; Kaufmann, E.; Clark, T.; Pople, J. A. *J. Am. Chem. Soc.* **1983**, *105*, 5930−5932.
(23) Akiba, K. Y.; Yamashita, M.; Yamamoto, Y.; Nagase, S. *J. Am. Chem. Soc.* **1999**, *121*, 10644−10645.
(24) Yamashita, M.; Yamamoto, Y.; Akiba, K. Y.; Hashizume, D.; Iwasaki, F.; Takagi, N.; Nagase, S. *J. Am. Chem. Soc.* **2005**, *127*, 4354−4371.
(25) Wang, Y. C.; Lv, J.; Zhu, L.; Ma, Y. M. *Phys. Rev. B* **2010**, *82*, 094116/1−094116/8.
(26) Wang, Y. C.; Miao, M. S.; Lv, J.; Zhu, L.; Yin, K. T.; Liu, H. Y.; Ma, Y. M. *J. Chem. Phys.* **2012**, *137*, 224108/1−224108/6.
(27) Lv, J.; Wang, Y. C.; Zhu, L.; Ma, Y. M. *J. Chem. Phys.* **2012**, *137*, 084104/1−084104/8.
(28) Wang, Y. C.; Lv, J.; Zhu, L.; Ma, Y. M. *Comput. Phys. Commun.* **2012**, *183*, 2063−2070. CALYPSO code is free for academic use. Please register at http://www.calypso.cn.
(29) Zhu, L.; Wang, H.; Wang, Y. C.; Lv, J.; Ma, Y. M.; Cui, Q. L.; Ma, Y. M.; Zou, G. T. *Phys. Rev. Lett.* **2011**, *106*, 145501/1−145501/4.
(30) Wang, H.; Tse, J. S.; Tanaka, K.; Iitaka, T.; Ma, Y. M. *Proc. Natl. Acad. Sci. U.S.A.* **2012**, *109*, 6463−6466.
(31) Wang, X. L.; Wang, Y. C.; Miao, M. S.; Zhong, X.; Lv, J.; Cui, T.; Li, J. F.; Chen, L.; Pickard, C. J.; Ma, Y. M. *Phys. Rev. Lett.* **2012**, *109*, 175502/1−175502/5.
(32) Zhao, Z. S.; Tian, F.; Dong, X.; Li, O.; Wang, Q. Q.; Wang, H.; Zhong, X.; Xu, B.; Yu, D. L.; He, J. L.; Wang, H. T.; Ma, Y. M.; Tian, Y. J. *J. Am. Chem. Soc.* **2012**, *134*, 12362−12365.
(33) Peng, F.; Miao, M. S.; Wang, H.; Li, Q. *J. Am. Chem. Soc.* **2012**, *134*, 18599−18605.
(34) Li, Q.; Zhou, D.; Zheng, W. T.; Ma, Y. M.; Chen, C. F. *Phys. Rev. Lett.* **2013**, *110*, 136403/1−136403/5.
(35) Kresse, G.; Furthmuller, J. *Phys. Rev. B* **1996**, *54*, 11169−11186.
(36) Togo, A.; Oba, F.; Tanaka, I. *Phys. Rev. B* **2008**, *78*, 134106/1−134106/9.
(37) Olinger, B. *J. Chem. Phys.* **1982**, *77*, 6255−6258.
(38) Giordano, V. M.; Datchi, F. *EPL* **2007**, *77*, 46002/1−46002/5.
(39) Liu, L. G. *Earth Planet. Sci. Lett.* **1984**, *71*, 104−110.
(40) Oganov, A. R.; Ono, S.; Ma, Y. M.; Glass, C. W.; Garcia, A. *Earth Planet. Sci. Lett.* **2008**, *273*, 38−47.
(41) Yamaguchi, T.; Yamamoto, Y.; Kinoshita, D.; Akiba, K. Y.; Zhang, Y.; Reed, C. A.; Hashizume, D.; Iwasaki, F. *J. Am. Chem. Soc.* **2008**, *130*, 6894−6895.
(42) Datchi, F.; Giordano, V. M.; Munsch, P.; Saitta, A. M. *Phys. Rev. Lett.* **2009**, *103*, 185701/1−185701/4.
(43) Woon, D. E; Dunning, T. H. *J. Phys. Chem. A* **2009**, *113*, 7915−7926.